Parma School of Theoretical Physics,

September 2006

LHC Physics and Montecarlo

Fabio Maltoni
maltoni@fyma.ucl.ac.be

Abstract

Simple questions, exercises, and web applications are proposed to enhance the comprehension of basic aspects of QCD, Monte Carlo, and LHC physics.

1 Introduction

This is a collection of tests, exercises, web applications useful for a first approach to understanding QCD, MonteCarlo's and they role in collider physics. The basic references where most of the exercises and examples were taken from are:

- "QCD and Collider Physics" by R.K. Ellis, J.W. Stirling, B.R. Webber (Cambridge Monographs, 1996). In addition some of the exercises reproposed here are from lectures given at CERN by B.R. Webber.

The simulations can be performed with the help of the `MadGraph/MadEvent` MonteCarlo, directly from the web or by downloading the main code at `http://madgraph.phys.ucl.ac.be`. In some sense they are meant to be the most active part (and therefore enjoyable) of the tutorials. Some little practice on how to use the web interface to the code is needed.

The available servers are three:

- UCL : **http://madgraph.phys.ucl.ac.be**
- IT : **http://madgraph.roma2.infn.it**
- US : `http://madgraph.hep.uiuc.edu` (old version)

Unless it is explicitly said, only the first two clusters should be used during the tutorial. Students should register to receive via e-mail a username and a password, that can be kept for future use. With this password one can generate codes for processes and dowload the code. To generate events on the clusters higher clearance has to be obtained (by sending a request by e-mail to one of the authors). For the tutorial we have activated a temporary account (User: Angels, Password: Demons) where web event generation is allowed.

2 MC 101

A complete set of exercises is given in the Mathematica Notebook
`http://maltoni.web.cern.ch/maltoni/MC101.nb`

2.1 Questions

1. Look at the plot of the cross sections at hadron colliders. What is the cross section for producing a Higgs of 120 GeV of mass? Suppose the Higgs decays into $b\bar{b}$ with branching ratio (=probability) one. What is the ratio signal over backround expected for such a channel at LHC?

2. How are the unknown higher order corrections usually estimated in QCD? Why?

2.2 Color flows

Using the 't Hooft double line formalism, whose rules are summarized in Fig. 1 calculate the color factors of the following diagrams shown in Fig. 2.

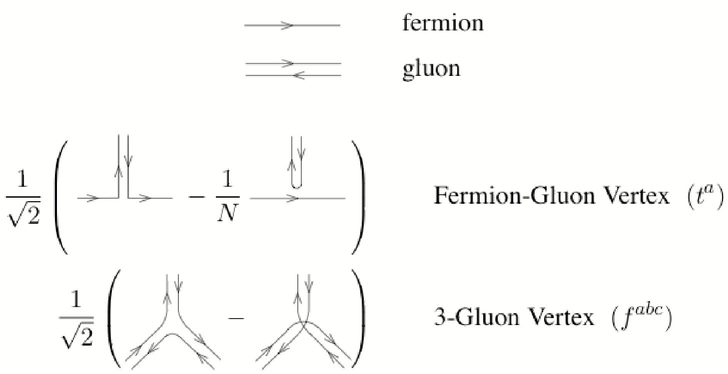

Figure 1: Double line Feynman rules useful to make fast and easy the evaluation of color factors.

In particular, compare the last color factor with that obtained from the diagram where the external gluon is replaced by a photon. In the former case the quark pair is in a color-octet state, while in the latter in a color-singlet state. Is the sign of the interaction between them the same?

2.3 Try MadGraph out

Logon to the MadGraph web site and register. Familiarize with the code by generating a few processes in QED and QCD trying to guess which diagrams appear. What is the minimum number of jets have to be asked for in e^+e^- collisions so that the triple gauge vertex appear?

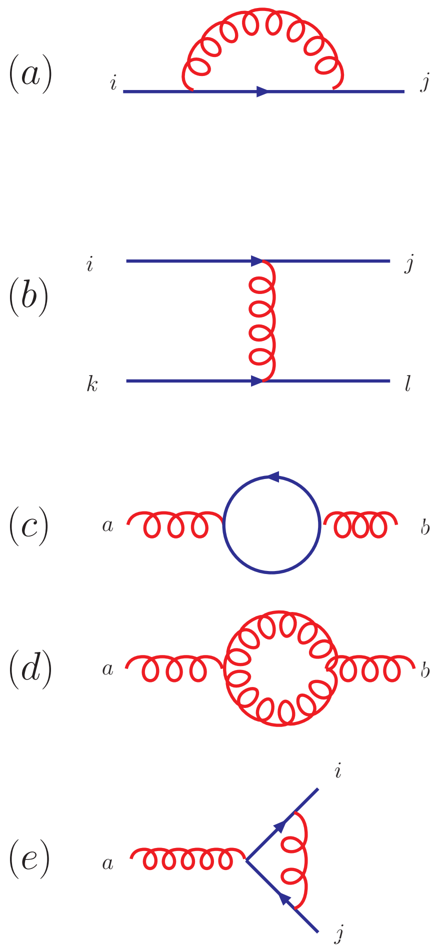

Figure 2: Sample of QCD diagrams.

Calculate the cross section for $u\bar{u} \to \gamma\gamma, u\bar{u} \to gg$, fixing the c.m.s energy at 100 GeV and leaving the acceptance cuts as in the default. Which one of the two processes gives as a larger cross section, taking in to account the difference in the couplings,i.e., setting $\alpha_S = \alpha_{EM}$?

3 Infrared safety and MC integrators

3.1 Questions

1. How should we intepret the leading order calculation for $\sigma(e^+e^- \to q\bar{q})$?
2. List the properties that a function of the four momenta has to enjoy to be an "infrared-safe" quantity.
3. Explain what is the physics leading to the idea of factorization.
4. Derive the soft Feynman rules for a qqg and ggg.
5. Show by explicit calculation that the form of the virtual corrections
$$\frac{d^2\sigma^{\mathrm{VIRT}}}{dEd\cos\theta} = -\sigma^{LO} C_F \frac{\alpha_S}{\pi} \int_0^{\sqrt{s/2}} \frac{dE'}{E'} \int_{-1}^{1} \frac{d\cos\theta'}{1-\cos^2\theta'} 2\delta(E')[\delta(1-\cos\theta')+\delta(1+\cos\theta')]+\dots \tag{1}$$
cancels the soft and collinear divergences present in $\sigma(e^+e^- \to q\bar{q}g)$.
6. Derive the amplitude for soft gluon emission from a $q\bar{q}g$ final state.
7. Show by explicit calculation in the example above that interference from different color flows is suppressed $1/N_c^2$. Generalize to any color flow.
8. Write down the definition of a two-jet cross section (Sterman-Weinberg) and see in which configurations $e^+e^- \to q\bar{q}g$ contributes to it.
9. Explain the idea of the subtraction method for NLO calculation.

3.2 $e^+e^- \to q\bar{q}$

(a) Derive the expression for the amplitude squared $e^+e^- \to q\bar{q}$,in terms of the invariants, s, t, u, for massless quarks. Include only photon exchange. Express it in terms of the c.m.s. variables $\cos\theta, \phi$ and write the differential cross section:
$$\frac{d\sigma}{d\cos\theta} = N_c(\sum_f Q_f^2)\frac{\pi\alpha^2}{2s}(1+\cos\theta^2)\,. \tag{2}$$
Which quarks should be included in the sum over flavors f?

(b) Include the diagram where a Z is exchanged and recall that the interaction vertex $q\bar{q}Z$ is given by:
$$\frac{-ig_w}{2\sqrt{2}}\gamma_\mu(V_f - A_f\gamma_5)\,, \tag{3}$$
and the axial and vector couplings of the fermions to the Z are
$$V_f = T_f^3 - 2Q_f\sin^2\theta_W\,, \qquad A_f = T_f^3\,, \tag{4}$$
with $T_f^3 = 1/2$for $f = \nu, u, \dots$ and $T_f^3 = -1/2$ for $f = e, d, \dots$.
What happens to the $\cos\theta$ distribution?

3.3 $e^+e^- \to q\bar{q}g$

(a) Show that the phase space for the unpolarized decay into three massless objects can be written as:

$$d\Phi_3 = \frac{1}{(2\pi)^5}\frac{s}{32}dx_1 dx_2 d\alpha d(\cos\beta)d\gamma \tag{5}$$

where s is the c.m.s. energy and $x_i = 2E_i/\sqrt{s}$ are the fractional energies for the quark and anti-quark.

(b) Calculate the matrix element squared for $e^+e^- \to q\bar{q}g$. Use the fact that we interested only in azimuthal averaged quantities and therefore we neglect angular correlations betweeen the initial state plane and the final state one, so we can write

$$|M|^2 = \frac{1}{s^2}L^{\mu\nu}H_{\mu\nu} \to \frac{1}{s^2}(L^{\mu\nu}g_{\mu\nu})(H^{\rho\sigma}g_{\rho\sigma}) \tag{6}$$

where $L^{\mu\nu}$ and $H^{\mu\nu}$ are the leptonic and hadronic tensors that come from the squaring of the the corresponding currents. The result to be be found is:

$$\sigma^{q\bar{q}g} = \sigma^{LO}C_F\frac{\alpha_S}{2\pi}\int dx_1 dx_2 \frac{x_1^2 + x_2^2}{(1-x_1)(1-x_2)} \tag{7}$$

where $\sigma^{LO} = N_c(\sum_f Q_f^2)4\pi\alpha^2/(3s)$.

(c) Perform the same calculation for a scalar gluon and verify that

$$\sigma^{q\bar{q}s} = \sigma^{LO}\int dx_1 dx_2 \frac{x_3^2}{2(1-x_1)(1-x_2)}\,. \tag{8}$$

3.4 Thrust distribution

The thrust is defined as:

$$T = \max_{\mathbf{n}}\frac{\sum_i |\mathbf{p}_i\cdot\mathbf{n}|}{\sum_i |\mathbf{p}_i|} \tag{9}$$

and in the case of $e^+e^- \to q\bar{q}g$ process it corresponds to the $\max\{x_i\}$, where the $x_i = 2E_i/\sqrt{s}$ are the energy fractions of each parton.

(a) Calculate the thrust distribution for a vector gluon:

$$\frac{d\sigma}{dT} = \int dx_1 dx_2 \frac{d\sigma}{dx_1 dx_2}\delta(T - \max\{x_i\})\,. \tag{10}$$

Convince yourself that the above result is obtained by integrating the differential cross section over the (JADE) countour in the (x_1, x_2) plane shown by the dashed line in Fig. 3. Compare your result with:

$$\frac{1}{\sigma}\frac{d\sigma}{dT} = C_F\frac{\alpha_S}{2\pi}\left[\frac{2(3T^2-3T+2)}{T(1-T)}\log\left(\frac{2T-1}{1-T}\right) - \frac{3(3T-2)(2-T)}{1-T}\right]\,. \tag{11}$$

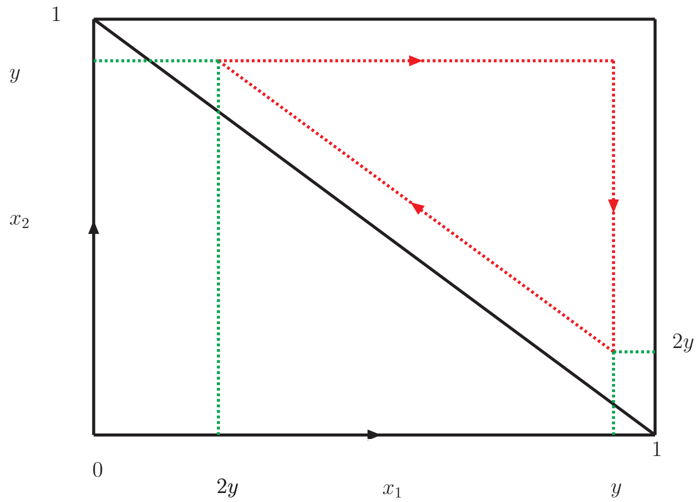

Figure 3: Countour in the (x_1, x_2) phase space plane corresponding to the JADE measure for jet definition. The differential cross section has to be integrated on the countour to obtain the thrust T. $y = T$.

(b) Calculate the thrust distribution for a scalar gluon and compare your result with:

$$\frac{1}{\sigma}\frac{d\sigma}{dT} = C_F \frac{\alpha_S}{2\pi}\left[\frac{9(2-T)T-8}{2(1-T)} + \log\left(\frac{2T-1}{1-T}\right)\right]. \tag{12}$$

(c) Plot the two distributions for $2/3 < T < 1$ in a log scale and compare with the data of Fig. 4. Why the QCD prediction at order $\mathcal{O}(\alpha_S)$ start to differ from the data when T approaches 1? What about at 2/3?

3.5 $e^+e^- \to Q\bar{Q}g$

(a) Compute the differential cross section for the case of massive final state using a program for symbolic calculations (such as `FORM` or `Mathematica+FeynCalc`) and compare your result with

$$\begin{aligned}\frac{1}{\sigma^{LO}}\frac{d^2\sigma}{dx_1 dx_2} = \quad & \frac{1}{\beta} C_F \frac{\alpha_S}{2\pi}\left[\frac{2(x_1+x_2-1-\rho/2)}{(1-x_1)(1-x_2)}\right. \\ & -\frac{\rho}{2}\left(\frac{1}{(1-x_1)^2} + \frac{1}{(1-x_2)^2}\right) \\ & \left. + \frac{1}{1+\rho/2}\frac{(1-x_1)^2+(1-x_2)^2}{(1-x_1)(1-x_2)}\right], \end{aligned} \tag{13}$$

where

$$\rho = \frac{4m^2}{s} \leq 1, \qquad \beta = \sqrt{1-\rho} \tag{14}$$

and σ^{LO} is defined as in Eq. (7).

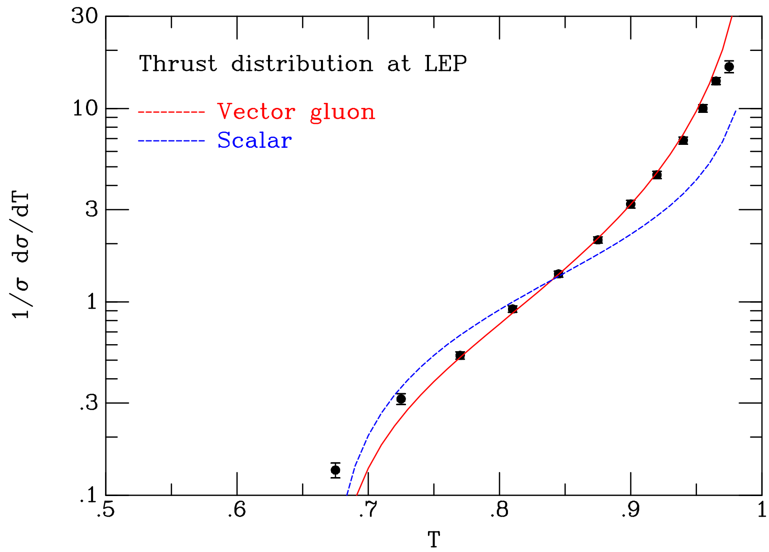

Figure 4: The thrust distribution measured at LEP, showing data from the DELPHI collaboration.

(b) Verify that the massless limit corresponds to Eq. (7). Study the soft and collinear limits. Is the collinear divergence still there? Write the soft and collinear approximation of the amplitude in the case the gluon is close to the quark:

$$\frac{1}{\sigma^{LO}}\frac{d^2\sigma}{dz d\theta^2} = C_F \frac{\alpha_S}{\pi}\frac{1}{z}\frac{\theta^2}{(\theta^2+\rho)^2} \tag{15}$$

where $z = 2E_g/\sqrt{s}$ is the energy fraction of the gluon and θ the angle between the gluon and the quark. Plot the behaviour of the matrix element in the massless and massive cases and compare with Fig. 5. Explain this behaviour in terms of angular momentum conservation.

3.6 Jet rates in the soft limit$^{(*)}$

(a) Derive the expression of the differential cross section for $e^+e^- \to q\bar{q}g$ in the soft limit, in the terms of the gluon energy E and the cosine of angle between the gluon and the quark (or anti-quark) $\cos\theta$:

$$\frac{d^2\sigma^{\text{REAL}}}{dE d\cos\theta} = \sigma^{LO} C_F \frac{2\alpha_S}{\pi}\frac{1}{E}\frac{1}{1-\cos^2\theta}\,. \tag{16}$$

(b) Without calculating the virtual contributions, guess their final form in order to cancel the soft and collinear divergences:

$$\frac{d^2\sigma^{\text{VIRT}}}{dE d\cos\theta} = -\sigma^{LO} C_F \frac{2\alpha_S}{\pi}\int_0^{\sqrt{s/2}}\frac{dE'}{E'}\int_{-1}^{1}\frac{d\cos\theta'}{1-\cos^2\theta'}\frac{1}{2}\delta(E')[\delta(1-\cos\theta')+\delta(1+\cos\theta')]+\ldots \tag{17}$$

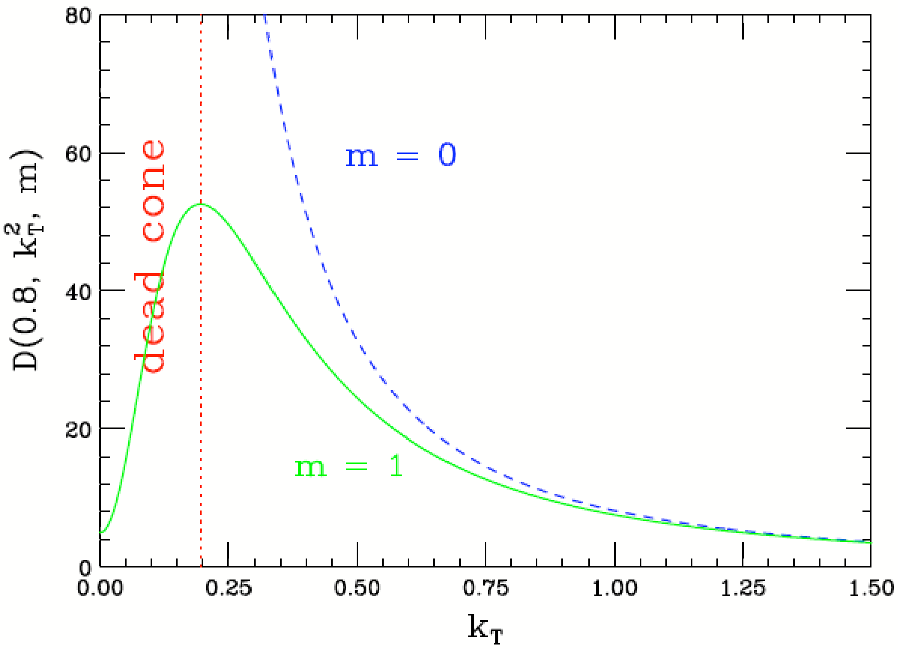

Figure 5: Dead cone: emission of collinear (soft) gluons from a massive quark is suppressed by angular momentum conservation.

(c) Define the two and three jet rates using the JADE measure, $y = M^2/s$ and calculate the two- and three-jet rates up to order α_S. First, identify the regions of the phase space contributing to the two jet rates

$$\begin{aligned} &\text{Region I} : E < y\sqrt{s} \qquad \text{and} \qquad 0 < \cos\theta < 1\,, \\ &\text{Region II} : E > y\sqrt{s} \qquad \text{and} \qquad 1 - \frac{y\sqrt{s}}{E} < \cos\theta < 1\,, \end{aligned} \tag{18}$$

and then perfom the integration:

$$\frac{\sigma_{2-\text{jet}}}{\sigma^{LO}} = \frac{1}{\sigma^{LO}}\left[2\int_{R_1} d\sigma^{\text{REAL}} + 2\int_{R_2} d\sigma^{\text{REAL}} + \int d\sigma^{\text{VIRTUAL}}\right] \tag{19}$$

Compare your result with:

$$\sigma_{2-\text{jet}} = \sigma^{LO}\left[1 - C_F\frac{\alpha_S}{\pi}\log^2 y + \ldots\right] \tag{20}$$

$$\sigma_{3-\text{jet}} = \sigma^{LO} C_F\frac{\alpha_S}{\pi}\log^2 y + \ldots \tag{21}$$

and, ignoring self-gluon interaction, exponentiate the above result to find the $\sigma_{(\text{n}+2)-\text{jet}}$ rate.

(d) Estimate the average number of the jets, $\langle n_{\text{jet}}\rangle$ and how the average number of particles in the final states (identify each particle with a jet at small y) scales with the c.m.s energy.

(e) Estimate the average invariant mass of the jets as a function of the c.m.s energy.

(f) Estimate the average thrust.

3.7 Thrust distributions

Use `MadGraph/MadEvent` to obtain the thrust distributions in $e^+e^- \to 3j$for a vector and a scalar gluon and compare your results with the analytic ones of Fig. 4. For details on the thrust definitions see Ex. 3.4.

3.8 $e^+e^- \to Q\bar{Q}g$

Use `MadGraph/MadEvent` and verify that there are no collinear divergences to be regulated and the cross section is finite with just a minimum cut on the energy of the gluon. Plot the behaviour of the cross sections as a function of the quark mass and verify that it has a logarithmic behaviour.

4 Evolution and Angular ordering

4.1 Questions

1. Rederive the DGLAP equations by following the argument given in the lectures
2. What is the Sudakov form factor?
3. Explain why by using the equation:

$$\frac{\Delta(t_1)}{\Delta(t_2)} = \mathcal{R} \tag{22}$$

where $\mathcal{R}$ is a uniformly distributed random number, the right distribution for the splitting is obtained.

4. Take the explicit form of the splitting functions given below and ignore $\delta(1-x)$ terms and the $()_+$ distributions. Set the color factors C_F, T_R, C_A to one. Prove they satisfy the SUSY relation

$$p_{gq} + p_{qq} = p_{qg} + p_{gg} \tag{23}$$

5. Present the physical explanation of the angular ordering.
6. Explain the Chudakov effect by angular ordering.
7. Explain pre-confinement.
8. Discuss the pattern of intra-jet and inter-jet radiation.

4.2 Splitting functions

Calculate the polarized splitting functions for $q \to qg$ and $g \to q\bar{q}$. For the spinor use the helicity basis. Explicit form of the spinors can be found in the ESW book.

4.3 DGLAP resums towers of logs

Show that the DGLAP equations resum a full tower of logarithms of Q^2.

4.4 Solve the DGLAP equations

Evolution is determined by the DGLAP equation, whose basic ingredients are the splitting functions.

(a) The plus-prescription is defined by

$$\int_0^1 dx f(x) g_+(x) \equiv \int_0^1 dx [f(x) - f(1)] g(x)\,. \tag{24}$$

Show that

$$\left(\frac{1+z^2}{1-z}\right)_+ = \frac{1+z^2}{(1-z)_+} + \frac{3}{2}\delta(1-z) \tag{25}$$

and

$$\left(\frac{z}{1-z} + \frac{1}{2}z(1-z)\right)_+ = \frac{z}{(1-z)_+} + \frac{1}{2}z(1-z) + \frac{11}{12}\delta(1-z)\,. \tag{26}$$

(b) The splitting functions are

$$\begin{aligned} P_{qq}(z) &= C_F\left(\frac{1+z^2}{1-z}\right)_+ && (27)\\ P_{qg}(z) &= T_R\left(z^2+(1-z)^2\right) && (28)\\ P_{gq}(z) &= C_F\frac{1+(1-z)^2}{z} && (29)\\ P_{gg}(z) &= 2C_A\left[\left(\frac{z}{1-z}+\frac{1}{2}z(1-z)\right)_+ + \frac{1-z}{z} + \frac{1}{2}z(1-z)\right] - \frac{2}{3}n_f T_R\delta(1-z) && (30)\end{aligned}$$

The anomalous dimensions are given by the moments of the splitting functions,

$$\begin{aligned} \gamma_{ij}(N,\alpha_S) &= \sum_{n=0}^{\infty}\gamma_{ij}^{(n)}(N)\left(\frac{\alpha_S}{2\pi}\right)^{n+1}, && (31)\\ \gamma_{ij}^{(0)}(N) &= \int_0^1 dz z^{N-1}P_{ij}(z)\,. && (32)\end{aligned}$$

Show that

$$\begin{aligned} \gamma_{qq}^{(0)}(N) &= C_F\left[-\frac{1}{2}+\frac{1}{N(N+1)}-2\sum_{k=2}^{N}\frac{1}{k}\right] && (33)\\ \gamma_{qg}^{(0)}(N) &= T_R\left[\frac{2+N+N^2}{N(N+1)(N+2)}\right] && (34)\\ \gamma_{gq}^{(0)}(N) &= C_F\left[\frac{2+N+N^2}{N(N+1)(N-1)}\right] && (35)\\ \gamma_{gg}^{(0)}(N) &= 2C_A\left[-\frac{1}{12}+\frac{1}{N(N-1)}+\frac{1}{(N+1)(N+2)}-2\sum_{k=2}^{N}\frac{1}{k}\right]-\frac{2}{3}n_f T_R\,. && (36)\end{aligned}$$

4.5 Soft cones

A soft function for a an emitter quark i, a soft gluon k, and a spectator anti-quark j is defined as

$$W_{(i)} \equiv \frac{1}{2}\left[\frac{\cos\theta_{jk}-\cos\theta_{ij}}{(1-\cos\theta_{ik})(1-\cos\theta_{jk})}+\frac{1}{1-\cos\theta_{jk}}\right]. \tag{37}$$

Prove that by averaging over the azimuthal angle, one obtains a positive definite quantity with the following properties:

$$\begin{aligned} \int\frac{d\phi_{ik}}{2\pi}W_{(i)} &= \frac{1}{1-\cos\theta_{ik}} \quad \text{if} \quad \theta_{ik}<\theta_{ij} && (38)\\ &= 0 \quad \text{otherwise.} && (39)\end{aligned}$$

Hint: An integral on a coplex contour is needed. Write $1 - \cos\theta_{jk} = a - b\cos\phi_{ik}$, where $a = 1 - \cos\theta_{ij}\cos\theta_{ik}$ and $b = \sin\theta_{ij}\sin\theta_{ik}$. Then define $z = \exp(i\phi_{ik})$ and rewrite the integral

$$I^{(i)} \equiv \int_0^{2\pi} \frac{\phi_{ik}}{2\pi} \frac{1}{1 - \cos\theta_{jk}} = \int \frac{dz}{(z - z_+)(z - z_-)}\,, \tag{40}$$

where the integration is done over the unit circle. Once the expression for $z_\pm$ are found, one realizes that only one pole, $z = z_-$ can lie insider the unit circle, so

$$I^{(i)} = \sqrt{\frac{1}{a^2 - b^2}} = \frac{1}{|\cos\theta_{ik} - \cos\theta_{ij}|}\,. \tag{41}$$

4.6 The BZ angle in $e^+e^- \to 4$jets: abelian vs non-abelian

Use `MadGraph/MadEvent` to produce two event samples, one for standard QCD and one with an abelian QCD model for

$$e^+e^- \to Z \to 4j\,. \tag{42}$$

Run the collision on the peak of the Z and set a minimum invariant mass for the jets of $m_{jj} > 10$ GeV. Plot the angle between the planes identified by the two lowest and to highest energy jets:

$$\cos\chi_{BZ} = \frac{(\mathbf{p}_1 \times \mathbf{p}_2) \cdot (\mathbf{p}_3 \times \mathbf{p}_4)}{|\mathbf{p}_1 \times \mathbf{p}_2||\mathbf{p}_3 \times \mathbf{p}_4|}\,. \tag{43}$$

Comparison should be made with the plots of Ref. `http://arxiv.org/abs/hep-ph/9503354`, where various implementation of the abelian models are discussed. Our web implementation include the emission of abelian gluons as possible partons leading to jets.
Explain your findings in terms of the polarized splitting functions.

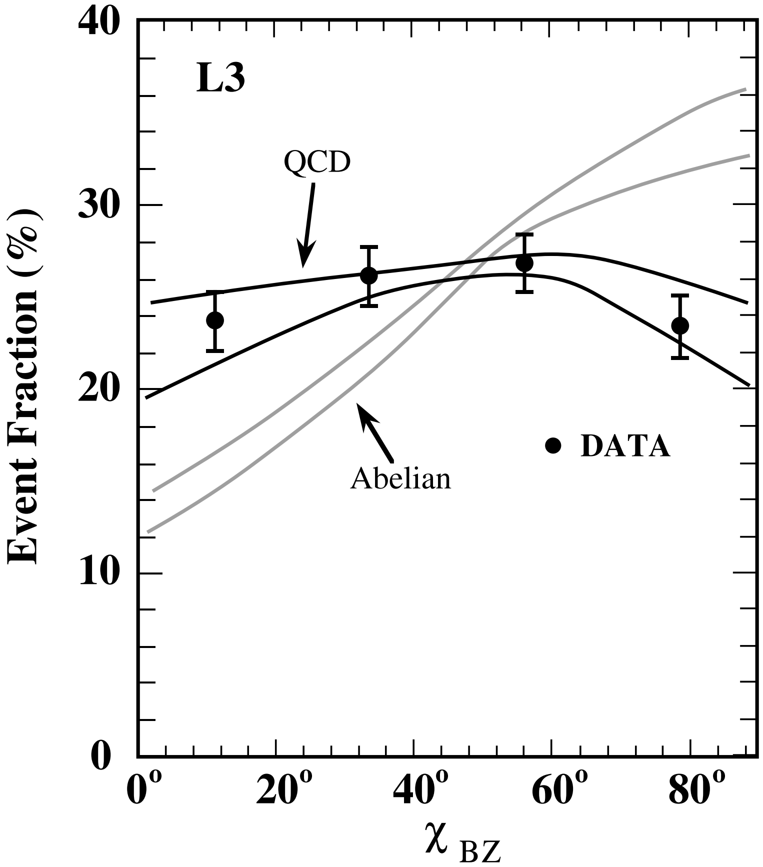

Figure 6: Distribution in the Bengtsson-Zerwas angle at LEP. Here the Abelian model includes only four-quark final states.

5 Hadron collisions

5.1 Basic kinematics for hadron collisions

The rapidity y and pseudo-rapidity η are defined as:

$$y = \frac{1}{2}\log\left(\frac{E+p_z}{E-p_z}\right) \tag{44}$$

$$\eta = -\log\left(\tan\left(\frac{\theta}{2}\right)\right), \tag{45}$$

where the z direction is that of the colliding beams.

(a) Verify that for a particle of mass m

$$E = \sqrt{m^2+p_T^2}\quad \cosh y \tag{46}$$

$$p_z = \sqrt{m^2+p_T^2}\quad \sinh y \tag{47}$$

$$p_T^2 = p_x^2+p_y^2\,. \tag{48}$$

(b) Prove that $\tanh\eta = \cos\theta$.

(c) Consider a set of particles produced uniformly in longitudinal phase space

$$dN = C\frac{dp_z}{E}\,. \tag{49}$$

Find the distribution in η.

(d) Prove that rapidity equals pseudo-rapidity, $\eta = y$ for a relativistic particle $E \gg m$.

(e) Prove that for Lorentz transformation (boost) in the beam (z) directions, the rapidity y of every particle is shifted by a constant y_0, related to the boost velocity. Find the relation between β and y_0 for a generic boost:

$$E' = \gamma(E - \beta p_z) \tag{50}$$
$$p'_z = \gamma(p_z - \beta E) \tag{51}$$
$$p'_x = p_x \tag{52}$$
$$p'_y = p_y \tag{53}$$
$$\gamma = \frac{1}{\sqrt{1-\beta^2}} \tag{54}$$

(f) Consider a generic particle X of mass M (such as a Z boson or a Higgs) produced on shell at the LHC , with zero transverse momentum, $pp \to X$. Find the relevant values of x_1, x_2 of the initial partons that can be accessed by producing such a particle. Compare your results with that of Fig. 7, considering the scale $Q = M$.

5.2 Jet kinematics

At the LHC, partons in the incoming beams (beam energy E_b=7 TeV) collide with a momementum fraction $x_{1,2}$ and produce two jets with negligible mass, transverse momentum p_T and rapidities $y_{3,4}$.

(a) Show that

$$x_1 = \frac{p_T}{\sqrt{s}}(e^{y_3} + e^{y_4}), \qquad x_2 = \frac{p_T}{\sqrt{s}}(e^{-y_3} + e^{-y_4})\,. \tag{55}$$

(b) Show that the invariant mass of the jet-jet system is

$$M_{JJ} = 2p_T\cosh\left(\frac{y_3 - y_4}{2}\right)\,, \tag{56}$$

and the centre-of-mass scattering angle is given by

$$\cos\theta^* = \tanh\left(\frac{y_3 - y_4}{2}\right)\,. \tag{57}$$

(c) Discuss the regions of $x_{1,2}, M_{JJ}$ and θ^* that can be studied at the LHC with a jet trigger of $p_T > 35$ GeV and $|y_{3,4}| < 3$.

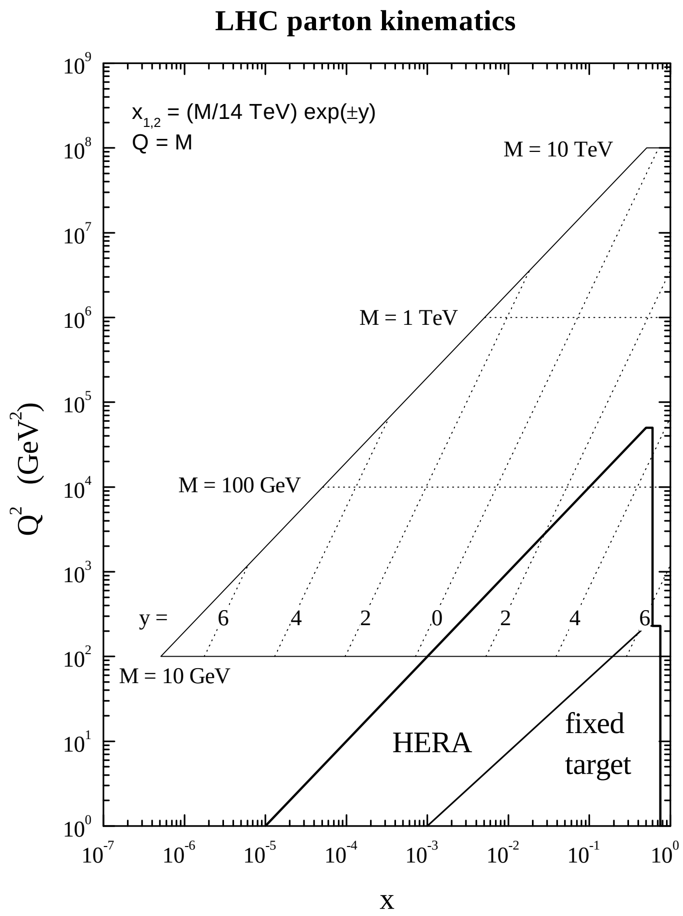

Figure 7: Range in x, Q accessible at the LHC.

5.3 Jet fraction from different parton combinations

Use `MadGraph/MadEvent` to obtain the relative contribution of $gg, qg + \bar{q}g, qq + q\bar{q}$ initial states to the jet E_T distribution as function of the E_T ($10 < E_T < E_{\max}/4$) at the Tevatron Run II ($p\bar{p}$ collisions at 1.96 TeV) and the LHC (pp collisions at 14 TeV). Compare with the results at the Tevatron, Run I shown in Fig. 8

5.4 Multijet production at the Tevatron$^{(*)}$

Use `MadGraph/MadEvent` to obtain the distributions of x_3, x_4 where $x_i = 2E_i/M_{3j}$ are the energy fraction of the jets normalized as $x_3 + x_4 + x_5 = 2$, with $x_3 > x_4 > x_5$, in three-jet events. Consider $p\bar{p}$ collisions at 1.8 TeV of c.m.s. Set the minimum p_T for the jets to 15 GeV, the maximum rapidity of 3.5 and the $\Delta R = 0.8$. Compare your results with the

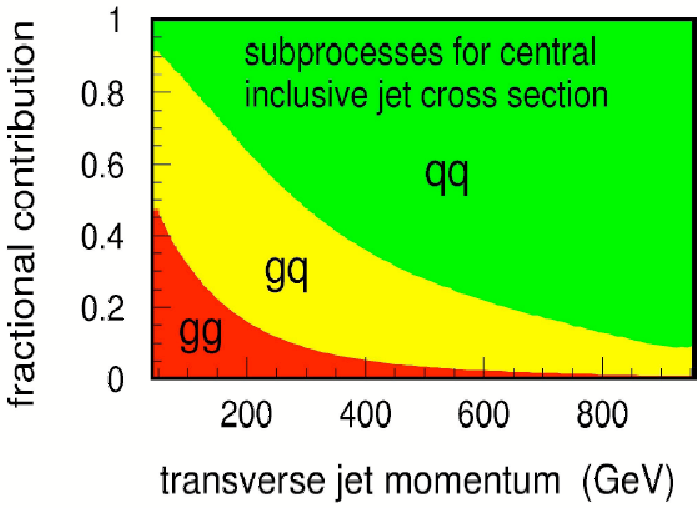

Figure 8: Plot showing the fraction of the jet E_T distribution initiated by different parton combinations.

experimental data from CDF, Run I, shown in Fig. 9.

5.5 $t\bar{t}$ production: Tevatron vs LHC

$t\bar{t}$ production at hadron collider come from both $q\bar{q}$ annhilation and gg fusion.

(a) Use the web interface of `MadGraph/MadEvent` to find the LO cross sections for $t\bar{t}$ production at Tevatron and LHC. Which initial parton contributions are dominating in the two cases?

(b) Use the web interface of `MadGraph/MadEvent` to find the cross sections for $t\bar{t}+1j$ production at the LHC. Select events for which the jet has $p_T > 20$ GeV and $|\eta| < 4$ (Is a ΔR cut needed to have a finite cross section?). Estimate the cross section and compare it with the LO result for $t\bar{t}$. Is the result reasonable? What's going on? Explain.

5.6 W rapidity asymmetry

The rapidity asymmetry $A_W(y)$ for $W^\pm$ production at a $p\bar{p}$ collider is defined as:

$$A_W(y) = \frac{d\sigma(W^+)/dy - d\sigma(W^-)/dy}{d\sigma(W^+)/dy + d\sigma(W^-)/dy}\,. \tag{58}$$

(a) Give an estimate of such asymmetry and show that it is proportional to the slope of $d(x)/u(x)$ evaluated at $x = M_W/\sqrt{s}$.

(b) Use the web interface of `MadGraph/MadEvent` to plot the rapidity distributions of the the charged leptons coming from $W^\pm$ decays at the Tevatron.

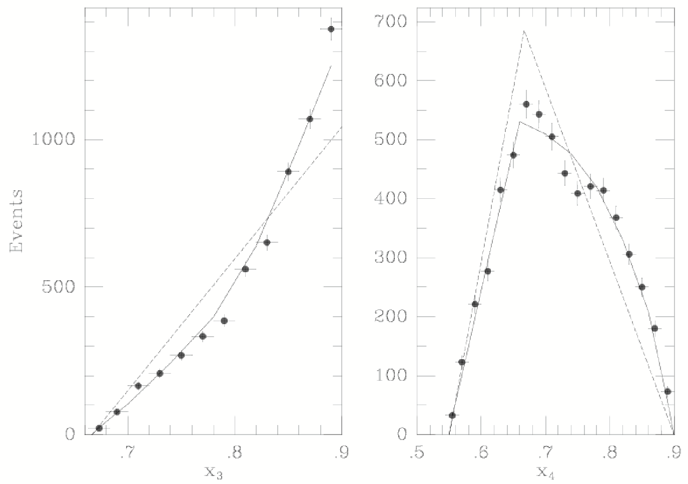

Figure 9: Distributions in the variables x_3 and x_4 in a sample of three jet events as measured by the CDF collaboration (Run I data), $p\bar{p}$ collisions at 1.8 TeV. The solid and dashed lines are the predicitons from QCD and phase space respectively.

Rapidity asymmetry is obviously not present at pp colliders. What could be alternative quantities sensitive to the pdf's?

5.7 Higgs discovery

Consider the processes:

$$pp \to t\bar{t}h \to t\bar{t}b\bar{b}\,, \qquad m_h = 120\,\text{GeV}\,, \tag{59}$$

$$pp \to h \to W^+W^- \to \mu^+\nu_\mu e^-\bar{\nu}_e, \qquad m_h = 165\,\text{GeV}\,. \tag{60}$$

Using the web interface of `MadGraph/MadEvent`

(a) Calculate their cross section at LO.

(b) Find out in the literature if the cross sections are known at NLO.

(c) Estimate the non-reducible backgrounds.

(d) By a careful analysis of the distributions, indentify the variables and the ranges where the signal is enhanced over the background.

6 Final project: Gluon fusion Higgs production at the LHC

In this section, one can follow all steps of the calculation of the cross section for $gg \to$ Higgs at LO with full top dependence and at NLO in the Higgs Effective Field theory. All the calculations shown here, including the MC for Higgs production at the LHC, are available in a series of Mathematica Notebooks that can be requested to the author.

6.1 Part I: $gg \to H$ via a top-quark loop

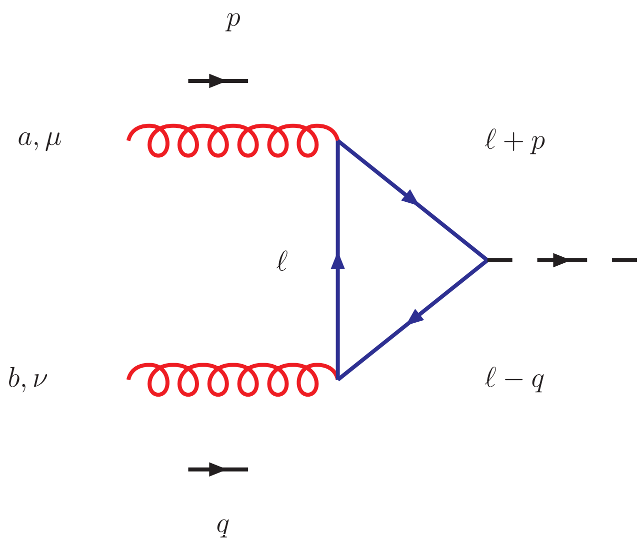

Figure 10: Representative Feynman diagram for the process $gg \to H$. Another diagram, the one with the gluons exchanged, contributes to the total amplitude.

The primary production mechanism for a Higgs boson in hadronic collisions is through gluon fusion, $gg \to H$, which is shown in Fig. 10. The loop contains all massive colored particles in the model. Consider only the top quark. To evaluate the diagram of Fig. 10 (there are actually two diagrams, the one shown and another one with the gluons exchanged. They give the same contribution so we'll just multiply our final result by two), use use dimensional regularization in $D = 4 - 2\epsilon$ dimensions.

(a) Using the QCD Feynman rules write the expression for the amplitude corresponding to the diagram of Fig. 10.

(b) Use the usual Feynman parametrization method to combine the denominators of the loop integral into one, using the following:

$$\frac{1}{ABC} = 2\int_0^1 dx \int_0^{1-x} \frac{dy}{[Ax + By + C(1-x-y)]^3} \tag{61}$$

and so the denominator becomes,

$$\frac{1}{\text{Den}} = 2\int dx\ dy \frac{1}{[\ell^2 - m_t^2 + 2\ell\cdot(px - qy)]^3}. \tag{62}$$

(c) Shift the integration momenta to $\ell' = \ell + px - qy$ so the denominator takes the form

$$\frac{1}{\text{Den}} \to 2\int dx\ dy \frac{1}{[\ell'^{\,2} - m_t^2 + M_H^2 xy]^3}. \tag{63}$$

(d) Evaluate the numerator of the loop integral in the shifted loop momentum. Use the fact that that for transverse gluons, $\epsilon(p)\cdot p = 0$ and so terms proportional to the external momenta, p_μ or q_ν, can be dropped. You should find that the trace is proportional to the quark mass. This can be easily understood as an effect of the spin-flip coupling of the Higgs. Gluons or photons do not change the spin of the fermion, while the Higgs does. If the quark circulating in the loop is massless then the trace vanishes due to helicity conservation. This is the reason why even when the Yukawa coupling of the light quark and the Higgs is enhanced (such as in SUSY or 2HDM with large $\tan(\beta)$), the contribution is anyway suppressed by the kimatical mass.

(e) Shift momenta in the numerator, drop terms linear in ℓ' and use the relation

$$\int d^dk \frac{k^\mu k^\nu}{(\ell^2 - C)^m} = \frac{1}{d} g^{\mu\nu} \int d^dk \frac{k^2}{(k^2 - C)^m} \tag{64}$$

to write the amplitude in the form

$$\begin{aligned} i\mathcal{A} &= -\frac{2g_s^2 m_t^2}{v}\delta^{ab}\int \frac{d^d\ell'}{(2\pi)^d}\int dxdy\Big\{g^{\mu\nu}\Big[m^2 + \ell'^2\Big(\frac{4-d}{d}\Big) + M_H^2(xy - \frac{1}{2})\Big] \\ &\quad + p^\nu q^\mu(1-4xy)\Big\}\frac{2dxdy}{(k'^2 - m_t^2 + M_H^2 xy)^3}\epsilon_\mu(p)\epsilon_\nu(q). \end{aligned} \tag{65}$$

(f) Compute the integral of Eq. 65 by using the well known formulas of dimensional regularization

$$\begin{aligned} \int \frac{d^dk}{(2\pi)^d}\frac{k^2}{(k^2 - C)^3} &= \frac{i}{32\pi^2}(4\pi)^\epsilon \frac{\Gamma(1+\epsilon)}{\epsilon}(2-\epsilon)C^{-\epsilon} \\ \int \frac{d^dk}{(2\pi)^d}\frac{1}{(k^2 - C)^3} &= -\frac{i}{32\pi^2}(4\pi)^\epsilon\Gamma(1+\epsilon)C^{-1-\epsilon}. \end{aligned} \tag{66}$$

You should find that your result is finite.

(g) Compare your result with the known result:

$$\mathcal{A}(gg \to H) = -\frac{\alpha_S m_t^2}{\pi v}\delta^{ab}\Big(g^{\mu\nu}\frac{M_H^2}{2} - p^\nu q^\mu\Big)\int dxdy\Big(\frac{1 - 4xy}{m_t^2 - m_H^2 xy}\Big)\epsilon_\mu(p)\epsilon_\nu(q). \tag{67}$$

(Note that we have multiplied by 2 in Eq. (67) to include the diagram where the gluon legs are crossed.) The Feynman integral of Eq. (67) can easily be performed to find an analytic result if desired. Note that the tensor structure could have been predicted from the start by using the fact that $p^\mu \mathcal{A}^{\mu\nu} = q^\nu \mathcal{A}^{\mu\nu} = 0$.

(h) Define $I(a)$ as

$$I(a) \equiv \int_0^1 dx \int_0^{1-x} dy \frac{1-4xy}{1-axy}. \tag{68}$$

and express the amplitude in terms of such an expression. Plot the function $I(a)$ and verify that it goes quickly to its limiting values when $a \to 0$ and $a \to \infty$. Numerically, the heavy fermion mass limit is an extremely good approximation even for $m \sim M_H$. From this plot we can also see that the contribution of light quarks to gluon fusion of the Higgs boson is irrelevant. In fact we have,

$$I(a) \longrightarrow_{a\to\infty} \sim -\frac{1}{2a}\log^2(a). \tag{69}$$

Therefore, for the Standard Model, only the top quark is numerically important when computing Higgs boson production from gluon fusion.

(i) It is particularly interesting to consider the case when the fermion in the loop is much more massive than the Higgs boson, $M_H \ll m_t$. In this case we find,

$$\mathcal{A}(gg \to H) \longrightarrow_{m>>M_H} -\frac{\alpha_S}{3\pi v}\delta^{ab}\Big(g^{\mu\nu}\frac{M_H^2}{2} - p^\nu q^\mu\Big)\epsilon_\mu(p)\epsilon_\nu(q). \tag{70}$$

We see that the production process $gg \to H$ is independent of the mass of the heavy fermion in the loop in the limit $M_H \ll m_t$. Hence it counts the number of heavy generations and is a window into new physics at scales much above the energy being probed. This is a contradiction of our intuition that heavy particles should decouple and not affect the physics at lower energy. The reason the heavy fermions do not decouple is, of course, because the Higgs boson couples to the fermion mass.

(l) Cross section at the LHC. Resonant production of a heavy Higgs can be found from the standard formula:

$$\begin{aligned}\hat\sigma &= \frac{1}{2s}\overline{|\mathcal{A}|^2}\frac{d^3P}{(2\pi)^3 2E_H}(2\pi)^4\delta^4(p+q-P)\\ &= \frac{1}{2s}\overline{|\mathcal{A}|^2}2\pi\delta(s-m_H^2),\end{aligned} \tag{71}$$

using

$$\delta^{ab}\delta^{ab} = N_c^2 - 1$$

$$\Big(g^{\mu\nu}\frac{M_H^2}{2} - p^\nu q^\mu\Big)^2 = \frac{m_H^4}{2} \tag{72}$$

$$\overline{|\mathcal{A}|^2} = \frac{1}{4}\frac{1}{(N_c^2-1)^2}|\mathcal{A}|^2\,. \tag{73}$$

Verify that the result is

$$\hat\sigma(gg \to H) = \frac{\alpha_S^2}{64\pi v^2} \mid I\Big(\frac{M_H^2}{m^2}\Big) \mid^2 \tau_0\delta(\tau - \tau_0)$$

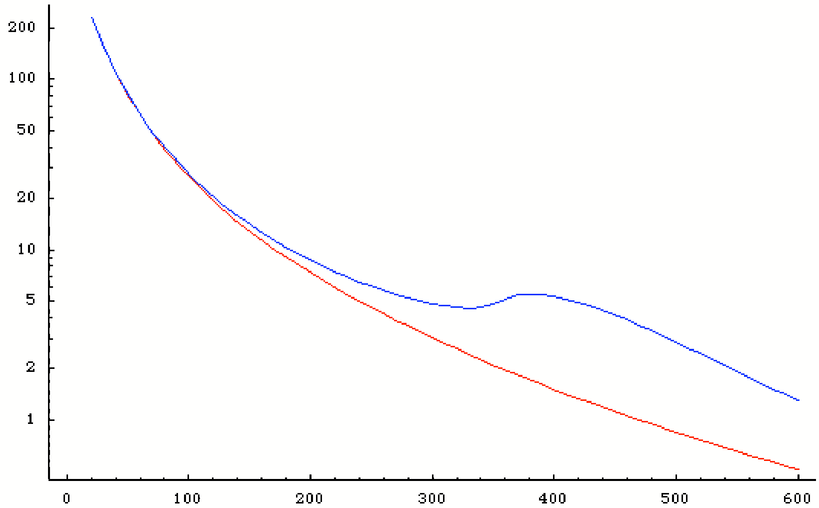

Figure 11: LO cross section for $pp \to H$ at LO at the LHC (pb) as a function of the Higgs mass (GeV).The red (lower) curve is the large top-mass limit, while the blue (upper) curve is the exact result.

where $s = x_1 x_2 S \equiv \tau S$ is the parton-parton energy squared, we have defined

$$z \equiv \frac{M_H^2}{s} = \frac{M_H^2}{\tau S} = \frac{\tau_0}{\tau} \tag{74}$$

with $\tau_0 = M_H^2/S$ and the integral I is defined by Eq. (68).

(m) To find the physical cross section we must integrate with the distribution of gluons in a proton,

$$\sigma(pp \to H) = \int_{\tau_0}^{1} dx_1 \int_{\tau_0/x_1}^{1} dx_2 g(x_1) g(x_2) \hat{\sigma}(gg \to H), \tag{75}$$

where $g(x)$ is the distribution of gluons in the proton. Perform the change of variables $x_1 \equiv \sqrt{\tau} e^y$, $x_2 \equiv \sqrt{\tau} e^{-y}$, and $\tau = x_1 x_2$. Find the Jacobian and the change of the integration limits and show that the result can be written as:

$$\sigma(pp \to H) = \frac{\alpha_S^2}{64\pi v^2} \mid I\left(\frac{M_H^2}{m^2}\right) \mid^2 \tau_0 \int_{\log\sqrt{\tau_0}}^{-\log\sqrt{\tau_0}} dy g(\sqrt{\tau_0} e^y) g(\sqrt{\tau_0} e^{-y}) \tag{76}$$

Often the above integral over the parton distribution is given the name of gluon-gluon parton luminosity.

(n) Using the pdf's from the CTEQ collaboration, CTEQ5L (Fortran,C or Mathematica) compute the gluon-gluon luminosity and the LO Higgs cross section at the LHC. Compare with the results shown in Fig. 11.

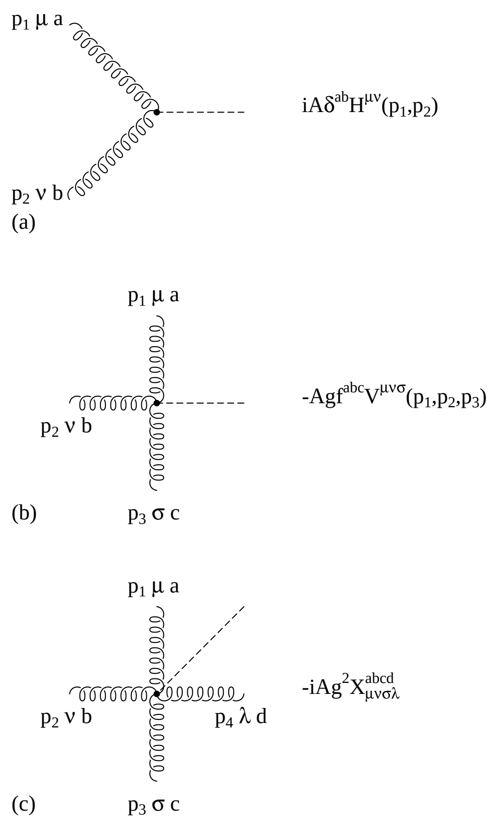

Figure 12: Feynman rules in the EFT where the top is integrated out. Gluon momenta are outgoing.

(n) Higgs Effective field theory.

A striking feature of our result for Higgs boson production from gluon fusion is that it is independent of the heavy quark mass for a light Higgs boson. In fact Eq. (70) can be derived from the effective vertex,

$$\begin{aligned} \mathcal{L}_{\rm eff} &= \frac{\alpha_S}{12\pi} G^A_{\mu\nu} G^{A\ \mu\nu} \left(\frac{H}{v}\right) \\ &= \frac{\beta_F}{g_s} G^A_{\mu\nu} G^{A\ \mu\nu} \left(\frac{H}{2v}\right)(1-\delta), \end{aligned}$$

where

$$\beta_F = \frac{g_s^3 N_H}{24\pi^2} \tag{77}$$

is the contribution of heavy fermion loops to the $SU(3)$ beta function and $\delta = 2\alpha_S/\pi$.[1]

[1] The $(1-\delta)$ term arises from a subtlety in the use of the low energy theorem. Since the Higgs coupling to the heavy fermions is $M_f(1+\frac{H}{v})\overline{f}f$, the counterterm for the Higgs Yukawa coupling is fixed in terms of the renormalization of the fermion mass and wavefunction. The beta function, on the other hand, is evaluated at $q^2=0$. The $1-\delta$ term corrects for this mismatch.

(N_H is the number of heavy fermions with $m >> M_H$.) The effective Lagrangian of Eq. (77) gives ggH, $gggH$ and $ggggH$ vertices and can be used to compute the radiative corrections of $\mathcal{O}(\alpha_S^3)$ to gluon production. The correction in principle involve 2-loop diagrams. However, using the effective vertices from Eq. (77), the $\mathcal{O}(\alpha_S^3)$ corrections can be found from a 1-loop calculation. To fix the notation we shall use

$$\mathcal{L}_{\rm eff} = -\frac{1}{4} A H G^A_{\mu\nu} G^{A\ \mu\nu}, \tag{78}$$

where $G^A_{\mu\nu}$ is the field strength of the SU(3) color gluon field and H is the Higgs-boson field. The effective coupling A is given by

$$A = \frac{\alpha_S}{3\pi v}\left(1 + \frac{11}{4}\frac{\alpha_S}{\pi}\right), \tag{79}$$

where v is the vacuum expectation value parameter, $v^2 = (G_F\sqrt{2})^{-1} = (246)^2\ \mathrm{GeV}^2$ and the α_S correction is included, as discussed above. The effective Lagrangian generates vertices involving the Higgs boson and two, three or four gluons. The associated Feynman rules are displayed in Fig. 12 The two-gluon–Higgs-boson vertex is proportional to the tensor

$$H^{\mu\nu}(p_1, p_2) = g^{\mu\nu} p_1 \cdot p_2 - p_1^\nu p_2^\mu. \tag{80}$$

The vertices involving three and four gluons and the Higgs boson are proportional to their counterparts from pure QCD:

$$V^{\mu\nu\rho}(p_1, p_2, p_3) = (p_1 - p_2)^\rho g^{\mu\nu} + (p_2 - p_3)^\mu g^{\nu\rho} + (p_3 - p_1)^\nu g^{\rho\mu}, \tag{81}$$

and

$$\begin{aligned} X^{\mu\nu\rho\sigma}_{abcd} &= f_{abe} f_{cde}(g^{\mu\rho} g^{\nu\sigma} - g^{\mu\sigma} g^{\nu\rho}) + f_{ace} f_{bde}(g^{\mu\nu} g^{\rho\sigma} - g^{\mu\sigma} g^{\nu\rho}) \\ &+ f_{ade} f_{bce}(g^{\mu\nu} g^{\rho\sigma} - g^{\mu\rho} g^{\nu\sigma}). \end{aligned} \tag{82}$$

6.2 Part II: $gg \to H$ @ NLO in the EFT

In this section we study the process $gg \to H$ at NLO, in the large top-quark mass limit. All results given below are in Conventional Dimensional Regularization (CDR). Using the effective Lagrangian for the gluon-gluon and gluon-Higgs interactions:

$$\mathcal{L}_{\rm eff} = -\frac{1}{4}\left(1 - \frac{\alpha_S}{3\pi}\frac{H}{v}\right) G^{\mu\nu} G_{\mu\nu} \tag{83}$$

one finds

$$\begin{aligned} \sigma_{\rm Born} &= \frac{\alpha_S^2}{\pi}\frac{m_H^2}{576 v^2 s}(1 + \epsilon + \epsilon^2)\mu^{2\epsilon}\,\delta(1 - z) \\ &\equiv \sigma_0\,\delta(1 - z)\,, \end{aligned} \tag{84}$$

where $z = m_H^2/s$ as defined previously. Note that we defined σ_0 as containing an explicit factor z. At NLO, for $gg \to H$, there are both virtual and real contributions. In the virtuals one should also take into account that the $\mathcal{L}_{\rm eff}$ gets corrected by the exchange of virtual gluons inside the top-quark loop, so that the interaction becomes:

$$\mathcal{L}_{\rm eff}^{\rm NLO} = \left(1 + \frac{11}{4}\frac{\alpha_S}{\pi}\right)\frac{\alpha_S}{3\pi}\frac{H}{v} G^{\mu\nu} G_{\mu\nu} \tag{85}$$

6.2.1 $gg \to H$: virtual corrections

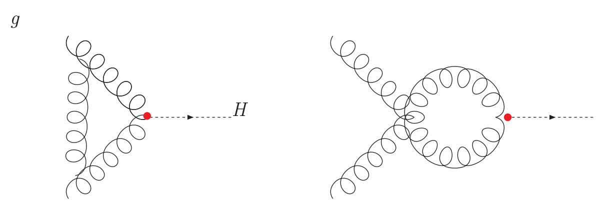

Figure 13: Feynman diagrams giving virtual contributions in the infinite top-quark mass limit

The non-zero virtual diagrams are two, the vertex correction and the bubble with the four gluon vertex. Their sum (plus the α_S corrections from Eq. (85) gives:

$$\sigma_{\rm virt} = \sigma_0\, \delta(1-z) \,\left[1 + \frac{\alpha_S}{2\pi} C_A \left(\frac{\mu^2}{m_H^2}\right)^{\epsilon} c_\Gamma \left(-\frac{2}{\epsilon^2} + \frac{11}{3} + \pi^2\right)\right], \tag{86}$$

where c_Γ where

$$c_\Gamma = (4\pi)^\epsilon \frac{\Gamma(1+\epsilon)\Gamma(1-\epsilon)^2}{\Gamma(1-2\epsilon)}. \tag{87}$$

6.2.2 Real Contribution: quark anti-quark initial state

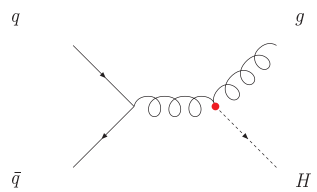

Figure 14: Feynman diagrams giving $q\bar{q}$ real contributions in the infinite top-quark mass limit. These contributions are finite.

This contribution, shown in Fig. 14 is finite and can be calculated directly in four dimensions. The amplitude is

$$\overline{|\mathcal{M}|^2} = \frac{4}{81} \frac{\alpha_S^3}{\pi v^2} \frac{(u^2+t^2) - \epsilon(u+t)^2}{s}, \tag{88}$$

to be integrated over the D-dimensional phase space

$$d\Phi_2 = \frac{1}{8\pi}\left(\frac{4\pi}{s}\right)^{\epsilon} \frac{1}{\Gamma(1-\epsilon)}\, z^\epsilon (1-z)^{1-2\epsilon}\, v^{-\epsilon}(1-v)^{-\epsilon} dv \tag{89}$$

where $v = 1/2(1+\cos\theta)$ and $z = M_H^2/s$ as usual. Using

$$t = -s(1-z)(1-v) \tag{90}$$
$$u = -s(1-z)v \tag{91}$$

and taking the limit $\epsilon \to 0$ gives:

$$\sigma_{\text{real}}(q\bar{q}) = \sigma_0 \frac{\alpha_S}{2\pi} \frac{64}{27} \frac{(1-z)^3}{z} \tag{92}$$

6.2.3 Real Contribution: quark gluon initial state

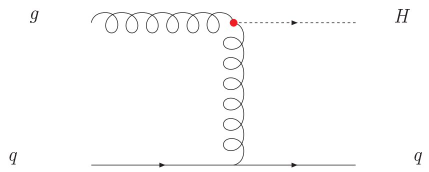

Figure 15: Feynman diagrams giving qg real contributions in the infinite top-quark mass limit.

Let us consider now the contribution from the diagrams with an initial quark, i.e., the process $gq \to Hq$. The amplitude is

$$\overline{|\mathcal{M}|^2} = -\frac{1}{54(1-\epsilon)} \frac{\alpha_S^3}{\pi v^2} \frac{(u^2+s^2) - \epsilon(u+s)^2}{t} \tag{93}$$

and integrating it over the D-dimensional phase space Eq. (89) we get

$$\sigma_{\text{real}} = \sigma_0 \frac{\alpha_S}{2\pi} C_F \left(\frac{\mu^2}{m_H^2}\right)^{\epsilon} c_\Gamma \left[-\frac{1}{\epsilon} p_{gq}(z) + z - \frac{3}{2}\frac{(1-z)^2}{z} + p_{gq}(z) \log\frac{(1-z)^2}{z}\right], \tag{94}$$

We perform the factorization of the collinear divergences adding the counterterm:

$$\sigma_{\text{c.t.}}^{\text{coll.}} = \sigma_0 \frac{\alpha_S}{2\pi} \left[\left(\frac{\mu^2}{\mu_F^2}\right)^{\epsilon} \frac{c_\Gamma}{\epsilon} P_{gq}(z)\right] \tag{95}$$

such that we get the result in the $\overline{\text{MS}}$ scheme (note that our definition of σ_0, Eq. (84), contains a factor z):

$$\begin{aligned} \sigma^{\overline{\text{MS}}}(qg) &= \sigma_{\text{real}} + \sigma_{\text{c.t.}}^{\text{coll.}} \\ &= \sigma_0 \frac{\alpha_S}{2\pi} C_F \left[p_{gq}(z) \log\frac{m_H^2}{\mu_F^2} + p_{gq}(z) \log\frac{(1-z)^2}{z} + z - \frac{3}{2}\frac{(1-z)^2}{z}\right]. \end{aligned} \tag{96}$$

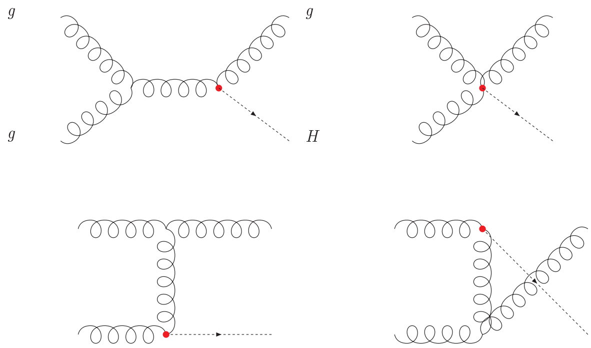

Figure 16: Feynman diagrams giving gg real contributions in the infinite top-quark mass limit.

6.2.4 Real Contribution: gluon-gluon initial state

For the real correction we have to integrate the $gg \to Hg$ amplitude

$$\overline{|\mathcal{M}|^2} = \frac{1}{24(1-\epsilon)^2}\frac{\alpha_S^3}{\pi v^2}\frac{(m_H^8+s^4+t^4+u^4)(1-2\epsilon)+\frac{1}{2}\epsilon(m_H^4+s^2+t^2+u^2)^2}{stu} \tag{97}$$

over the D-dimensional phase space Eq.(89). This gives

$$\begin{aligned}\sigma_{\rm real} &= \sigma_0\,\frac{\alpha_S}{2\pi}C_A\left(\frac{\mu^2}{m_H^2}\right)^\epsilon c_\Gamma\,\left[\left(\frac{2}{\epsilon^2}+\frac{2}{\epsilon}\frac{b_0}{C_A}-\frac{\pi^2}{3}\right)\delta(1-z)\right.\\ &\quad -\frac{2}{\epsilon}p_{gg}(z)-\frac{11}{3}\frac{(1-z)^3}{z}-4\frac{(1-z)^2(1+z^2)+z^2}{z(1-z)}\log z\\ &\quad \left.+\,4\frac{1+z^4+(1-z)^4}{z}\left(\frac{\log(1-z)}{1-z}\right)_+\right].\end{aligned} \tag{98}$$

Once again the above result is looks the same in both regularization schemes.
Adding it up, we get:

$$\begin{aligned}\sigma_{\rm real}+\sigma_{\rm virt} &= \sigma_{\rm Born}+\sigma_0\,\frac{\alpha_S}{2\pi}C_A\left(\frac{\mu^2}{m_H^2}\right)^\epsilon c_\Gamma\,\left[\left(\frac{11}{3}\frac{2}{\epsilon}\frac{b_0}{C_A}+\frac{2\pi^2}{3}\right)\delta(1-z)\right.\\ &\quad -\frac{2}{\epsilon}p_{gg}(z)-\frac{11}{3}\frac{(1-z)^3}{z}-4\frac{(1-z+z^2)^2}{z(1-z)}\log z\\ &\quad \left.+\,8\frac{(1-z+z^2)^2}{z}\left(\frac{\log(1-z)}{1-z}\right)_+\right].\end{aligned} \tag{99}$$

At variance with the Drell-Yan process, there is a left-over divergence proportional to $\delta(1-z)$. This is associated to the renormalization of the strong coupling. Using Eq. (115) and Eq. (**??**) we can write the following counterterm:

$$\sigma^{\rm UV}_{\rm c.t.} = 2\,\sigma_{\rm Born}\frac{\alpha_S}{2\pi}\,\left[-\left(\frac{\mu^2}{\mu_{\rm UV}^2}\right)^\epsilon c_\Gamma\frac{b_0}{\epsilon}\right] \tag{100}$$

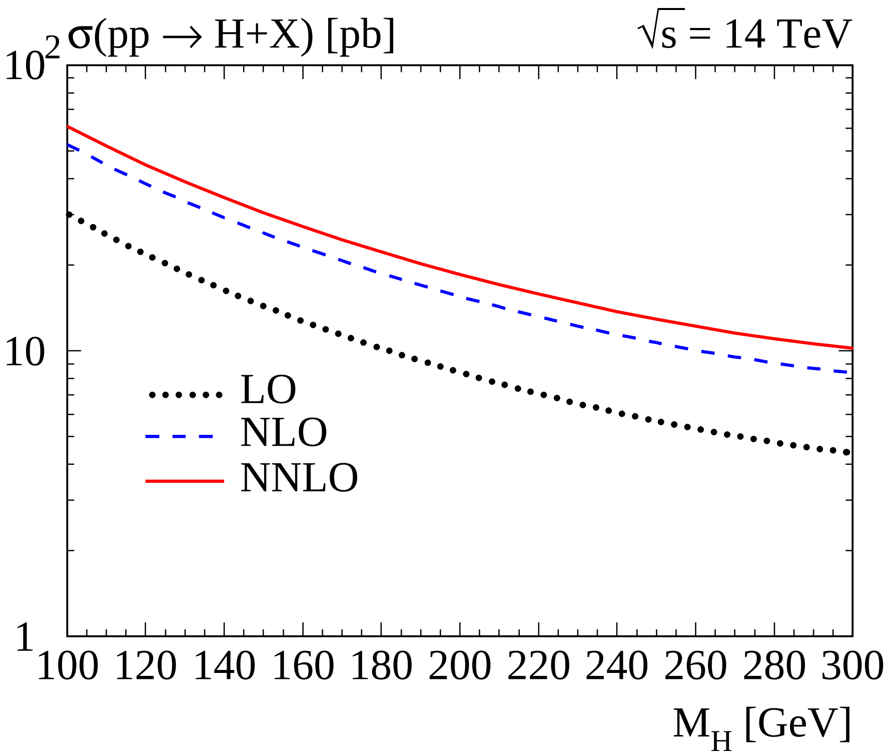

Figure 17: Cross section for Higgs procduction from gluon fusion at the LHC.

The factorization of the collinear divergence is handled is the usual way adding the counterterm:

$$\sigma^{\text{coll.}}_{\text{c.t.}} = 2\,\sigma_0 \frac{\alpha_S}{2\pi}\left[\left(\frac{\mu^2}{\mu_F^2}\right)^{\epsilon}\frac{c_\Gamma}{\epsilon}P_{gg}(z)\right] \tag{101}$$

such that we get the usual result in the $\overline{\text{MS}}$ scheme (note that our definition of σ_0, Eq. (84), contains a factor z):

$$\begin{aligned}\sigma^{\overline{\text{MS}}}(gg) \quad = \quad & \sigma_0\,\frac{\alpha_S}{2\pi}C_A\left[\left(\frac{11}{3}+\frac{2}{3}\pi^2-2\frac{b_0}{C_A}\log\frac{m_H^2}{\mu_{\text{UV}}^2}\right)\delta(1-z)\right. \\ & -\frac{11}{3}\frac{(1-z)^3}{z}+2p_{gg}\log\frac{m_H^2}{\mu_F^2}-4\frac{(1-z+z^2)^2}{z(1-z)}\log z \\ & \left.+\,8\frac{(1-z+z^2)^2}{z}\left(\frac{\log(1-z)}{1-z}\right)_+\right]\,. \end{aligned} \tag{102}$$

6.2.5 Results

Results are shown in Figs. 17 and 18

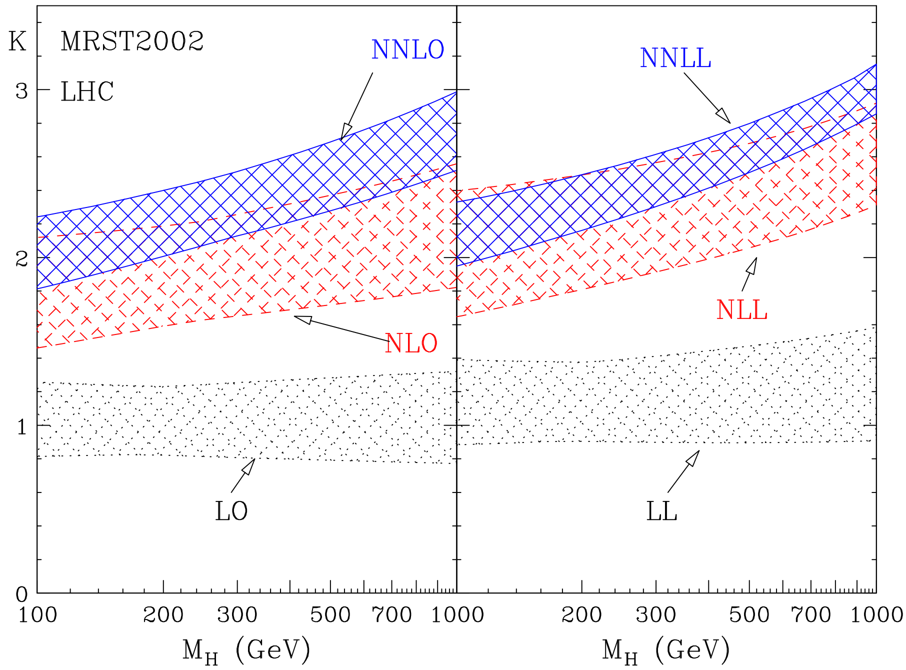

Figure 18: K-factors for Higgs production from gluon fusion at the LHC.

6.2.6 Appendix

We define the 4-dimensional splitting functions as in (4.94) of the ESW book:

$$P_{qq}(z) = C_F\, p_{qq}(z) = C_F \left[\frac{1+z^2}{(1-z)_+} + \frac{3}{2}\delta(1-z)\right] \tag{103}$$
$$P_{qg}(z) = T_R\, p_{qg}(z) = T_R \left[z^2 + (1-z)^2\right] \tag{104}$$
$$P_{gq}(z) = C_F\, p_{gq}(z) = C_F \left[\frac{1+(1-z)^2}{z}\right] \tag{105}$$
$$P_{gg}(z) = C_A\, p_{gg}(z) = 2C_A \left[\frac{z}{(1-z)_+} + \frac{1-z}{z} + z(1-z)\right] + b_0\, \delta(1-z)\,, \tag{106}$$

where $b_0 = 11/6\, C_A - 2n_f T_F/3$. We also define the following quantities as the extension of the splitting functions in Conventional Dimensional Regularization :

$$P_{ij}^{\rm CDR}(z) = P_{ij}(z) + \epsilon P_{ij}^{\epsilon}(z) \tag{107}$$

where

$$P_{qq}^{\epsilon}(z) = C_F\, p_{qq}^{\epsilon}(z) = -C_F(1-z) \tag{108}$$
$$P_{qg}^{\epsilon}(z) = T_R\, p_{qg}^{\epsilon}(z) = -T_R 2z(1-z) \tag{109}$$
$$P_{gq}^{\epsilon}(z) = C_F\, p_{gq}^{\epsilon}(z) = -C_F z \tag{110}$$
$$P_{gg}^{\epsilon}(z) = 0 \tag{111}$$

Factorization of the collinear divergences is performed through the addition of the following counterterm for each parton in the initial state:

$$\mathrm{CT}^{\mathrm{CDR}} \;=\; \sigma_0^{\mathrm{CDR}} \;\; \frac{\alpha_S}{2\pi} \left[\left(\frac{\mu^2}{\mu_F^2} \right)^{\epsilon} \frac{c_\Gamma}{\epsilon} P_{ij}(z) \right] \tag{112}$$

where $\sigma_0^{\mathrm{SCHEME}}$ is the LO cross section and its value depends on the scheme (see the example for Drell-Yan)]. In CDR, when there is a collinear divergence, the cross section behaves as

$$\sigma_{\mathrm{real}}^{\mathrm{coll}} \sim -\frac{1}{\epsilon} P_{ij}^{\mathrm{CDR}}(z) \sigma_0^{\mathrm{CDR}} \; + \text{other terms} \,. \tag{113}$$

Adding the counterterm (**??**), leaves a finite part

$$\sigma_{\mathrm{real}}^{\overline{\mathrm{MS}}} \sim -P_{ij}^{\epsilon}(z) \; (\sigma_0^{\mathrm{CDR}}|_{\epsilon\to 0}) \; + \text{other terms} \,. \tag{114}$$

7 Strong coupling renormalization

In this section we just state the rule. The $\overline{\mathrm{MS}}$ ultraviolet counterterm for the scattering amplitude at 1-loop is:

$$\frac{n}{\epsilon} \left[-b_0 \, \frac{\alpha_S}{4\pi} \; c_\Gamma \mathcal{A}^{\mathrm{tree}} \right] \,, \tag{115}$$

where $b_0 = 11/6 \, C_A - 2 n_f T_F / 3$ and n is the order of the tree-level amplitude in g_s. The above counterterm is defined in CDR.